

Speed Detection of Motor by Using Rotor Position and Speed Detector

Young-Choon Kim¹, Moon-Taek Cho^{2*} and Ok-Hwan Kim¹

¹*Dept. of Mechanical & Automotive Engineering, Kongju National University, 275 Buda-dong, Seobuk-gu, Cheonam-si, Chungnam, 31080, Korea*

²*Dept. of Electrical & Electronic Engineering, Daewon University College, 316 Daehak Road, Jecheon, Chungbuk, 27135, Korea*

{yckim59,owkim}@kongju.ac.kr, mtcho@mail.daewon.ac.kr,

Abstract

As a speed control device for motor control, optical encoders are frequently employed, while resolvers are used when mounting of the encoder onto a motor is structurally difficult. Although the resolvers are disadvantageous in the price aspect compared with the encoders, they are useful in the case of control based on the positions of stimulus as absolute positions of the rotor are detected. For an encoder attached to a motor, magnetic detection method is used primarily in comparison with encoders of general optical method. When the controller controls based on positions of the rotor as in synchronous motors, position information is a very important element. Therefore, since a technique for accurate estimation of the rotor position should be used in the case of using an encoder of low resolution when a synchronous motor is used as a structure of directly connecting a traction motor to the wheel, the resolver has been employed in the present study. Thus, in the present article, the minimum hardware of filter was used as a method to detect rotary speed of the motor according to the resolver, and a speed detector by digital method according to a program has been presented.

Keywords: *Speed control, Encoder, Resolver, Rotor position, Traction motor*

1. Introduction

Resolver and encoder can be differentiated by the fundamental difference of possibility status in the direct detection function for absolute positions. Resolver calculates rotary direction and rotary speed according to position changes of the rotor by direct detection of rotor's absolute positions. Encoder should calculate relative positions according to detection of the rotating direction by 2-phase pulse and to the number of pulses counted from the moment of reference pulse. That is why an encoder with addition of 3 separate encoder tracks is used to provide information on absolute positions of the rotor in control of AC servo, *etc.* using an encoder.

For estimation of speeds, methods of using an observer are known. While there are excellent characteristics in the range of estimation by the observer even if there is an error of various integers, problems occur in the case of inertia of the object system applied or great variation of loads.

For position detection in motors, encoders of optical method are mainly used in general, while encoders or resolvers employing a magnetic method are being used when vibration, *etc.* are severe. Traction motor for driving vehicles is connected to a truck supporting wheels, requiring solid mechanical characteristics for the encoder to detect speeds under operation conditions such as vibration, *etc.* Thus, magnetic detection method is mainly used for the encoders attached to motors in comparison with encoders of general optical

* Corresponding Author

methods. When the controller controls on the basis of rotor positions as in a synchronous motor, the position information is a very important element. Since a technique for accurate estimation of the rotor position should be used in the case of using an encoder of low resolution when a synchronous motor is used as a structure for directly connecting a traction motor to the wheel, the resolver was employed in the present study.

Input for the resolver is the excitation current for signal output, with coupling in the structure of a rotary transformer. Also, in the case of resolver employed, signals of 10[kHz] are supposed to be used, and the position information as an output signal is also outputting the signals modulated to the frequency of inputted excitation current. Therefore, positions should be calculated by demodulation to cosine and sine waveforms of 2-phase output as position information for the rotor and by removing noise included in these waveforms.

In the present article, an observer for estimation of position and speed was employed, and the interface for the resolver employed to measure position and speed was comprised of an oscillator to excite the resolver and analog amplifier, signal-generating circuit to drive the sampler, a filter circuit for resolver signals, a sampling circuit, and a block having functions of transmission of analog signals and A/D conversion for digital observation system.

Also, as a process for calculation of fundamental waves by using DFT, the rotor positions were directly calculated according to the demodulated 2-phase signals, and a resolving power of more than 12 bits has been obtained for the speed estimated by PI controller.

2. Estimation of Speed and Observer

All printed material, including text, illustrations, and charts, must be kept within the parameters of the 8 15/16-inch (53.75 picas) column length and 5 15/16-inch (36 picas) column width. Please do not write or print outside of the column parameters. Margins are 3.3cm on the left side, 3.65cm on the right, 2.03cm on the top, and 3.05cm on the bottom. Paper orientation in all pages should be in portrait style.

To estimate speed, position and load of the rotor when controlling the motor, equations of motion for the motor are used. When the motor has a rotary inertia load, the relationship between turning effect of the motor and load torque, rotary speed of the rotating body as well as position of the rotor are as shown in the equation (1).

$$\begin{cases} \frac{d\theta}{dt} = \omega \\ \frac{d\omega}{dt} = \frac{1}{J}(T - T_L) \end{cases} \quad (1)$$

In the motor, accelerations defined by a difference between turning effect and load torque as a function of load inertia are determined. Since positions of the rotor are detected, the observer to observe position and speed of the rotor may be obtained as in the equation (2).

$$L(y - Cx) = \begin{bmatrix} l_1 \\ l_2 \end{bmatrix} (\theta - \hat{\theta}) \quad (2)$$

When the position error is made to converge to the detected position by feedback, observation of speeds is possible. Equation (3) is obtained by the equation (1) and the equation (2).

$$\begin{bmatrix} \dot{\hat{\theta}} \\ \dot{\hat{\omega}} \end{bmatrix} = \begin{bmatrix} \hat{\omega} + l_1(\theta - \hat{\theta}) \\ \frac{T}{J} - \frac{T_L}{J} + l_2(\theta - \hat{\theta}) \end{bmatrix} \quad (3)$$

The observer of the equation (3) is represented by the block diagram as shown in Figure 1.

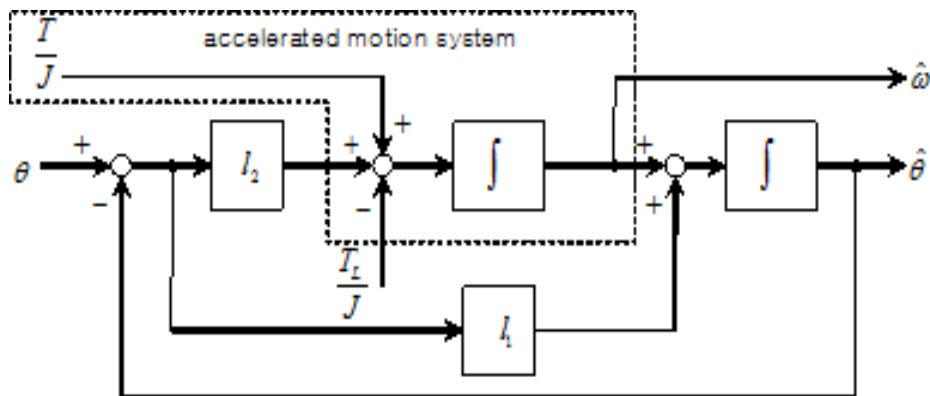


Figure 1. Estimation of Rotary Speed and Rotor Position

The dotted line part in Figure 1 shows an acceleration block for estimating speeds $(T - T_L)/J$ where the acceleration becomes $(T - T_L)/J$. As it is determined by torque and load inertia of the motor, the block is changed more slowly as the inertia is increased. Unless this block has the relationship between torque and load torque of the motor equivalent to the actual system, normal errors for the position come to exist. Position error for the rotor gives rise to the equation (4).

$$\tilde{\theta} = \theta - \hat{\theta} \tag{4}$$

Where, the extent of position errors is related to l_2 when l_2 is proportionately controlled so as to control performance of the observer. To eliminate errors of the equation (4) in the steady state, the equation (5) can be obtained by using PI controller instead of l_2 so that the observer converges to the rotor position detected in Figure 1.

$$l_2 = l_p + \frac{l_i}{s} \tag{5}$$

From the equation (5), the block diagram of Figure 2 can be produced.

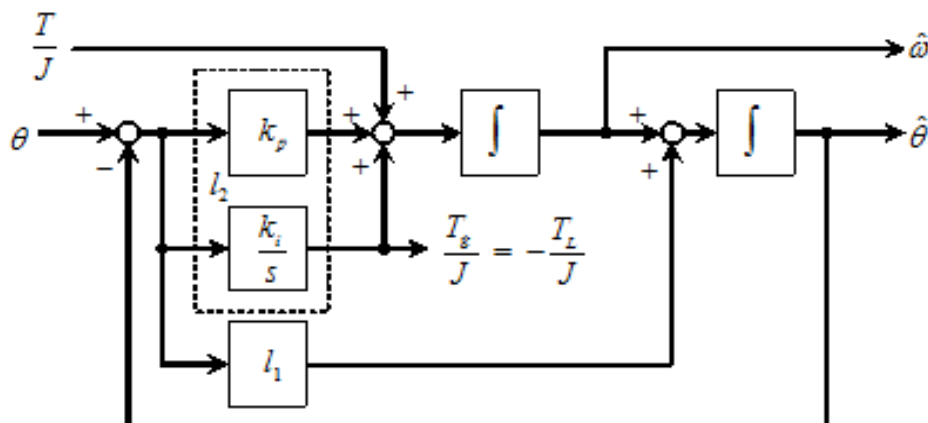


Figure 2. Observer Equipped with PI Controller

When the observer of Figure 2 is assumed to converge to the system, the output of the integration controller (T_g/J) may be considered as the physical output having the opposite sign from that of deceleration component (T_L/J) since there is no position error of the

rotor in the steady state. Load torque of the motor may have a load as shown by the equation (6).

$$T_L = T_a + a\omega \quad (6)$$

In the equation (6), $a\omega$ is the general load torque as a physical quantity proportional to speeds, T_a is a physical quantity unrelated to speeds and may be considered to correspond to torque due to the gradient of road or rail in the case of traction motor for driving vehicles. Since the equation (7) as shown in Figure 2 becomes the equation (8), the equation (9) may be obtained by substituting the equation (8) for the equation (3).

$$\frac{T_g}{J} = -\frac{T}{J} \quad (7)$$

$$\begin{cases} -\frac{\hat{\tau}_l}{J} = \frac{\hat{\tau}_g}{J} = l_i(\theta - \hat{\theta}) \\ \hat{\omega} = \frac{T}{J} + \frac{\hat{\tau}_g}{J} + l_p(\theta - \hat{\theta}) \end{cases} \quad (8)$$

$$\begin{bmatrix} \hat{\theta} \\ \hat{\omega} \\ \frac{\hat{\tau}_g}{J} \end{bmatrix} = \begin{bmatrix} 0 & 1 & 0 \\ 0 & 0 & 1 \\ 0 & 0 & 0 \end{bmatrix} \begin{bmatrix} \hat{\theta} \\ \hat{\omega} \\ \frac{\hat{\tau}_g}{J} \end{bmatrix} + \begin{bmatrix} 0 \\ 1 \\ 0 \end{bmatrix} \frac{T}{J} + \begin{bmatrix} l_1 \\ l_p \\ l_i \end{bmatrix} (\theta - \hat{\theta}) \quad (9)$$

For the observer according to Figure 2 and the equation (9), measurements of speed and position become possible even if the acceleration block for estimation of speeds is not the same as the actual system. However, when the speed estimator becomes accurately equivalent to the actual system, estimation of load torque is also possible in the accelerated state. In the load-free state, the acceleration characteristics are determined by load inertia and torque of the motor. Therefore, the actual system can be depicted if the acceleration block is controlled in the state without position errors when the method of Figure 2 is used. Since the equation (9) may be represented by the equation (10), the characteristic equation of an observer such as the equation (11) becomes the equation (11) and the equation (12).

$$\hat{x} = A\hat{x} + Bu + L(y - C\hat{x}) \quad (10)$$

$$|\lambda - (A - LC)| = \begin{vmatrix} \lambda + l_1 & -1 & 0 \\ k_p & \lambda & -1 \\ k_i & 0 & \lambda \end{vmatrix} = 0 \quad (11)$$

$$\lambda^3 + l_1\lambda^2 + k_p\lambda + k_i = 0 \quad (12)$$

Considering the equation (13) to obtain the root for the characteristic equation, gain for the state feedback becomes the equation (14).

$$(\lambda + a_1)(\lambda + a_2)(\lambda + a_3) = 0 \quad (13)$$

$$\begin{cases} l_1 = a_1 + a_2 + a_3 \\ k_p = (a_1a_2 + a_2a_3 + a_1a_3) \\ k_i = a_1a_2a_3 \end{cases} \quad (14)$$

3. Motion Equation of Rotating Body

Considering motion equation for the motor in the relationship for the equation (9) and the equation (10), the equation (15) is obtained.

$$\begin{cases} \dot{x} = Ax + Bu \\ y = Cx \end{cases} \quad (15)$$

The original system for the observer of the equation (9) may be considered as the system shown in the equation (16).

$$\begin{cases} \begin{bmatrix} \dot{\theta} \\ \dot{\omega} \\ \dot{T_g} \\ J \end{bmatrix} = \begin{bmatrix} 0 & 1 & 0 \\ 0 & 0 & 1 \\ 0 & 0 & 0 \end{bmatrix} \begin{bmatrix} \theta \\ \omega \\ T_g \\ J \end{bmatrix} + \begin{bmatrix} 0 \\ 1 \\ 0 \end{bmatrix} \frac{T}{J} \\ y = [1 \ 0 \ 0] \begin{bmatrix} \theta \\ \omega \\ T_g \\ J \end{bmatrix} \end{cases} \quad (16)$$

4. Design of Detector

Since excitation voltages are to use sine waves, sine waves are generated by Wien bridge, which are amplified to be used as excitation voltages. Since the detector(resolver) is attached to the motor driven by a power converter to output signals including noise caused by leakage flux, *etc.* the use of filter and differential input circuit to remove the noise is essential. Therefore, the excited signals and the output signals will have a phase lag, and the maximum output voltages should be sampled irrespective of transfer function of the filter. However, in the present study, a circuit operated for the fixed filter was designed by using the block as shown in Figure 3.

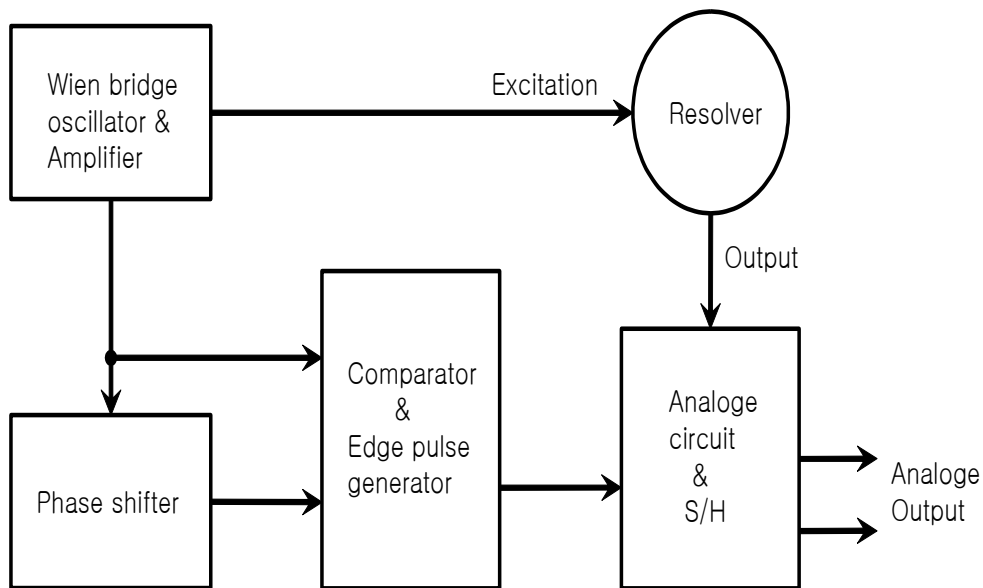


Figure 3. Resolver Signal Processing

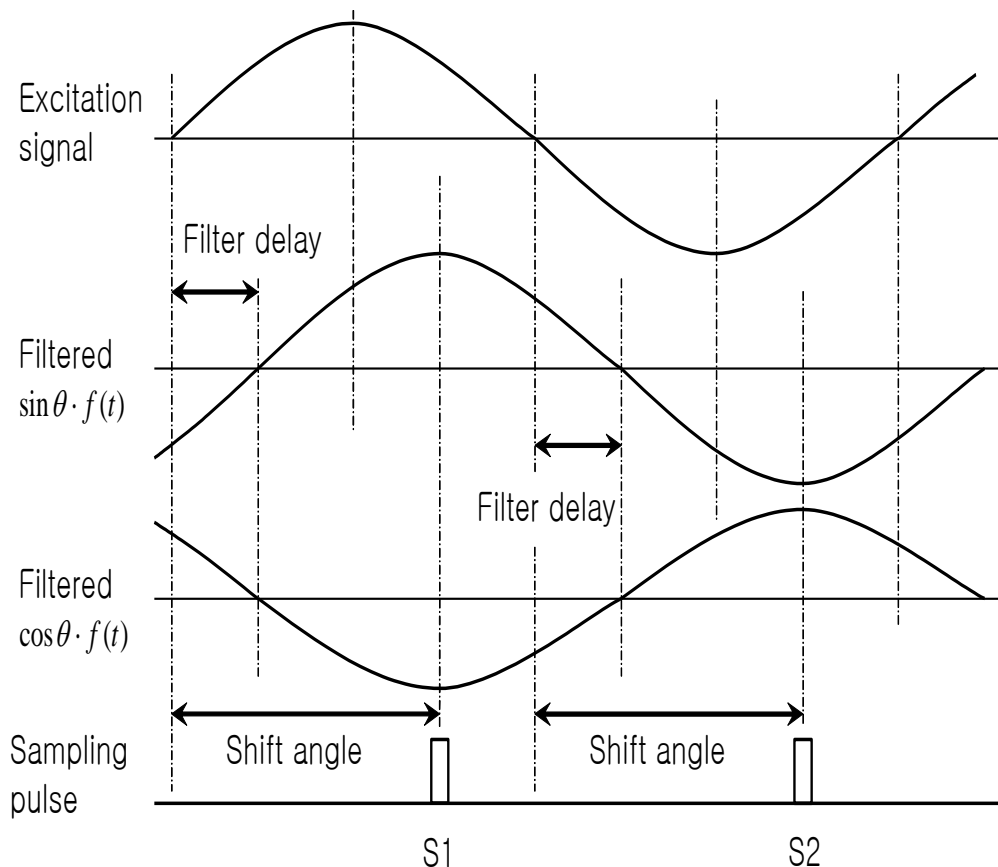


Figure 4. Lag of Filter and Sampling

Figure 4 describes a method of demodulating outputs of the resolver by the sampling method. If the maximum values are to be sampled in the delayed signals by using a filter, sampling pulse considering lag of the filter is required as shown in Figure 4. When the excitation voltage is made as a reference, output signals of the resolver after filter become a delayed waveform as shown in Figure 4. Used for generation of sampling pulses is the analog method of moving the phase of waveform for excitation voltage up to the point of sampling pulse generated. Figure 8 shows a block diagram for detection processing of rotor position and speed.

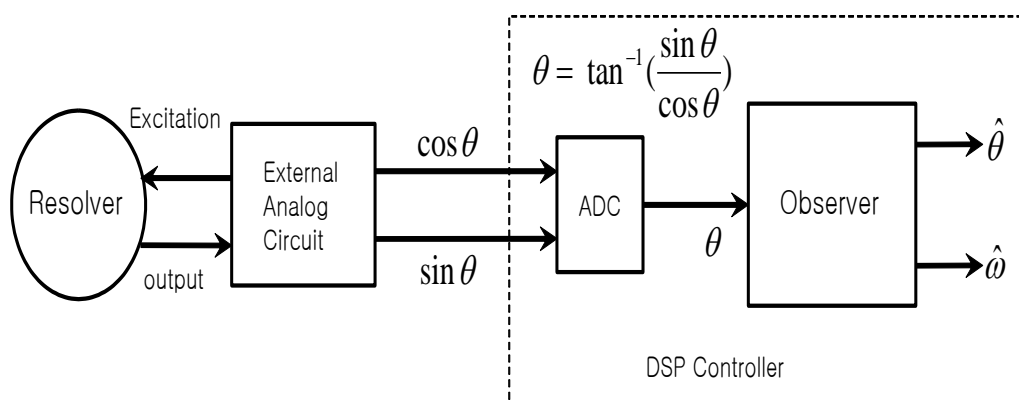


Figure 5. Detection of Rotor Positions and Speeds

5. Estimation Position and Speed

The waveforms of cosine and sine obtained from the resolver are inputted in the controller as digital signals, with position and rotary speed of the rotor being calculated by the program. Position of the rotor is calculated as shown by the equation (17).

$$\theta = \tan^{-1} \left(\frac{\sin \theta}{\cos \theta} \right) \quad (17)$$

Since the noise is included in the rotor position according to the equation (17), inaccuracy in position information cannot be excluded. Since a method for estimation of positions becomes necessary from here, motion equations for the motor are considered. The rotating body with inertia is represented by the equation (18).

$$\begin{cases} \frac{d\theta}{dt} = \omega \\ \frac{d\omega}{dt} = \frac{1}{J} (T - T_L) \end{cases} \quad (18)$$

Since the measurable variable in the equation (18) is the rotor position calculated by the equation (17), the whole-dimension observer for the system of the equation (18) is represented by the equation (19).

$$\begin{cases} \frac{d\ddot{\theta}}{dt} = \omega + g_1(\theta - \hat{\theta}) \\ \frac{d\hat{\omega}}{dt} = \frac{1}{J} (T - T_L) + g_2(\theta - \hat{\theta}) \end{cases} \quad (19)$$

The second speed equation in the equation (18) and the equation (19), respectively, includes inertia of the rotating body, torque of the motor and load torque, while the information on these cannot be included in the detector. Therefore, to erase the terms related to inertia and torque, position and rotary speed are estimated by using the PI controller for the state feedback as in the equation (20).

$$\begin{cases} \frac{d\theta}{dt} = \omega + g_1(\theta - \hat{\theta}) \\ \frac{d\hat{\omega}}{dt} = \left(g_p + \frac{g_i}{s} \right) (\theta - \hat{\theta}) \end{cases} \quad (20)$$

Considering the equation (21) on the right side of the second equation of the equation (20), the equation (23) is obtained.

$$G = g_i(\theta - \hat{\theta}) \quad (21)$$

$$\begin{cases} \frac{d\ddot{\theta}}{dt} = \hat{\omega} + g_1(\theta - \hat{\theta}) \\ \frac{d\hat{\omega}}{dt} = \hat{G} + g_p(\theta - \hat{\theta}) \\ \frac{d\hat{G}}{dt} = g_i(\theta - \hat{\theta}) \end{cases} \quad (22)$$

G in the equation (22) becomes acceleration related to inertia and turning effect of the rotary system. When acceleration is not accurately estimated even if the rotor position converges to the actual system in the steady state, there can exist the cases where errors are accompanied in the states of acceleration and deceleration with rotary speeds being varied. Consequently, feedback gains of the equation (22) need to be determined by repeated experiments.

The observer of the detector for estimation of rotor position and rotary speed according to the equation (20) or the equation (22) is represented by the block diagram as shown in Figure 6.

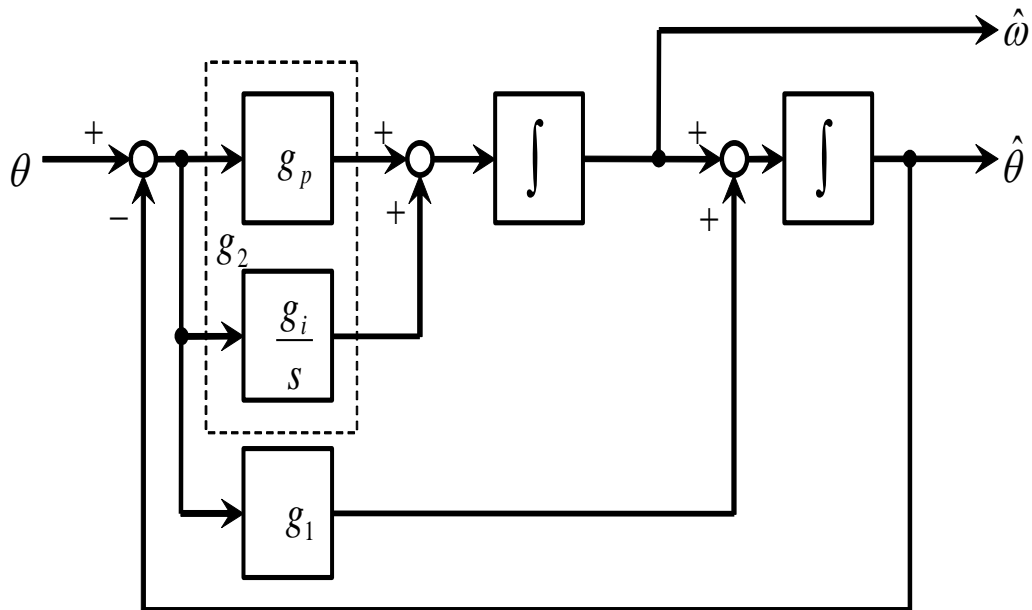


Figure 6. Detection of Position and Speed of Rotor

5. Adjustment and Measurement of Gain for Estimator

Figure 7 shows measurement of PWM outputs and excited signals applied to the resolver after filter. Sampling was conducted at 10[us], and frequency of excited signals set at 10[kHz]. To adjust PI gains of the speed estimator, responses were observed by varying rotor positions. Speed and position were measured for the maximum value of 5[V].

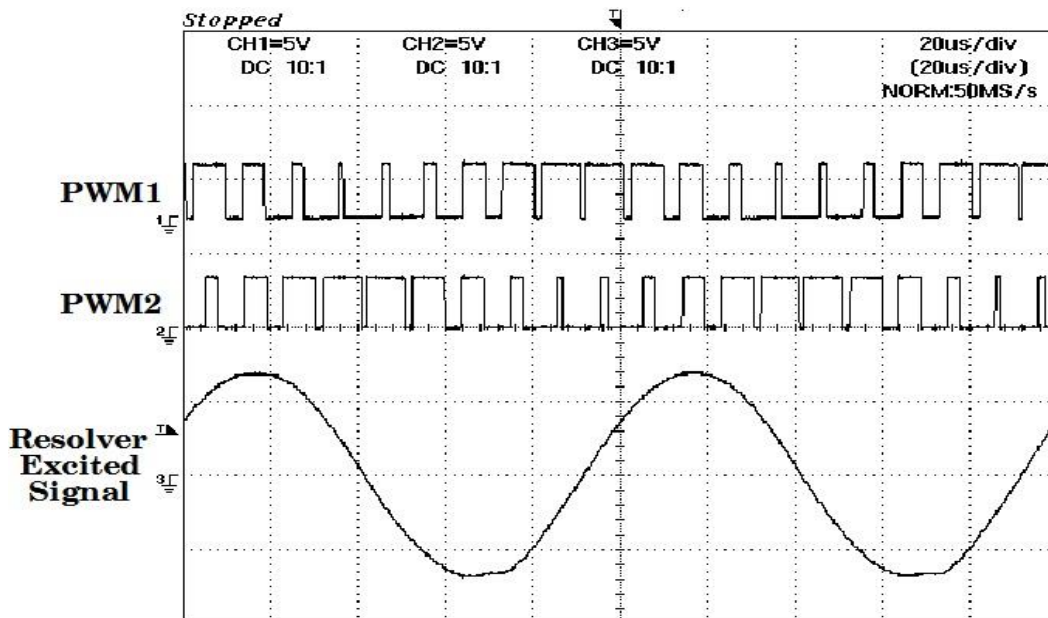


Figure 7. Excited Signal for Resolver

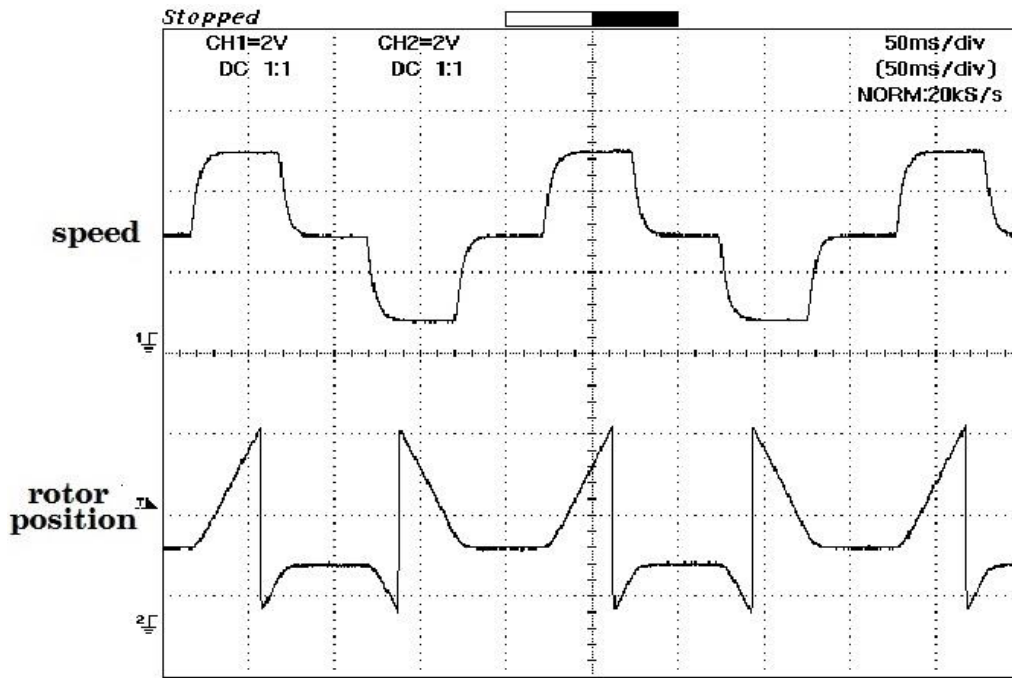


Figure 8. Step Response

Figure 8 shows the response of the estimator for step changes in speed with the measurement range of ± 1200 [rpm], while Figure 9 shows the measurement for estimation of speed and position upon acceleration and deceleration. Figure 10 shows the observation of precision in the stopped state. In 16-bit data, the lower 6 bit was measured for speed, and the lower 4 bit for position. Speed shows the precision of 12 bit, while position estimation for the rotor shows the precision of about 15 bit.

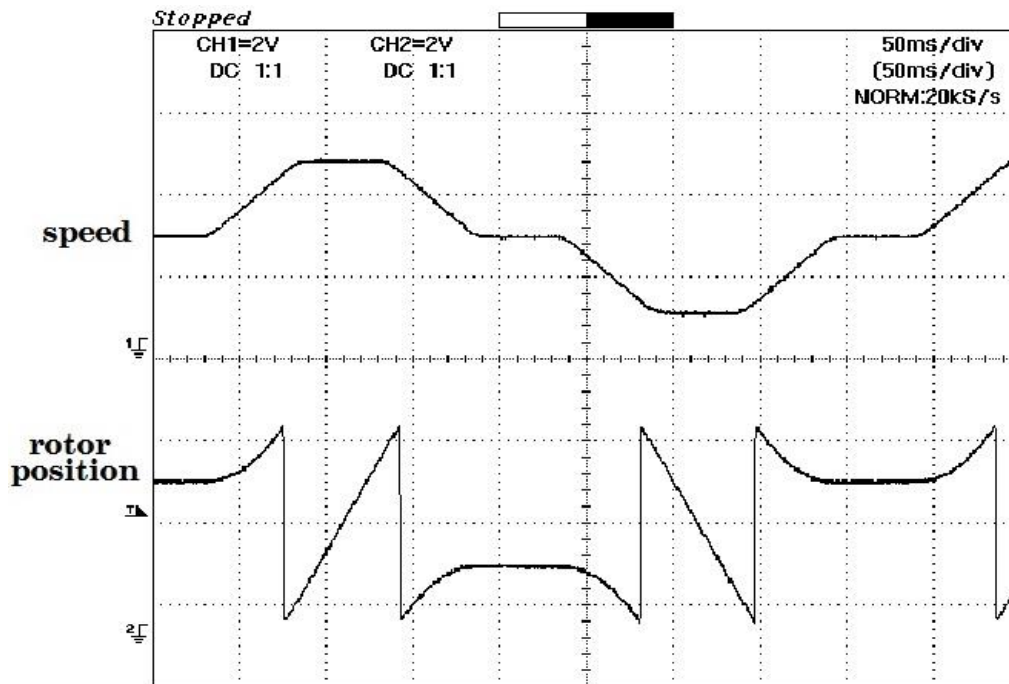


Figure 9. Speed Response

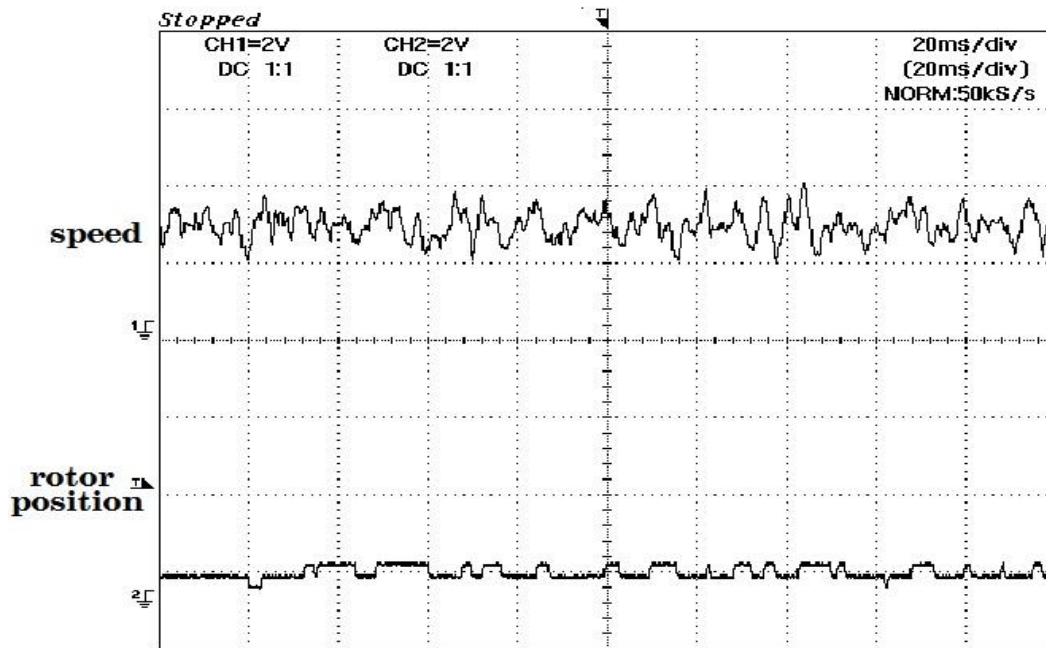


Figure 10. Output when Rotor is Stopped

According to the experimental results, the precision was observed to be improved, although responsiveness was lowered with a decrease in the gain of the estimator.

Figure 11 shows the measurement of excitation voltages and output waveforms when the excitation frequency of the resolver was made to be 11[KHz]. The bottom figure shows a magnification for a part of the top figure.

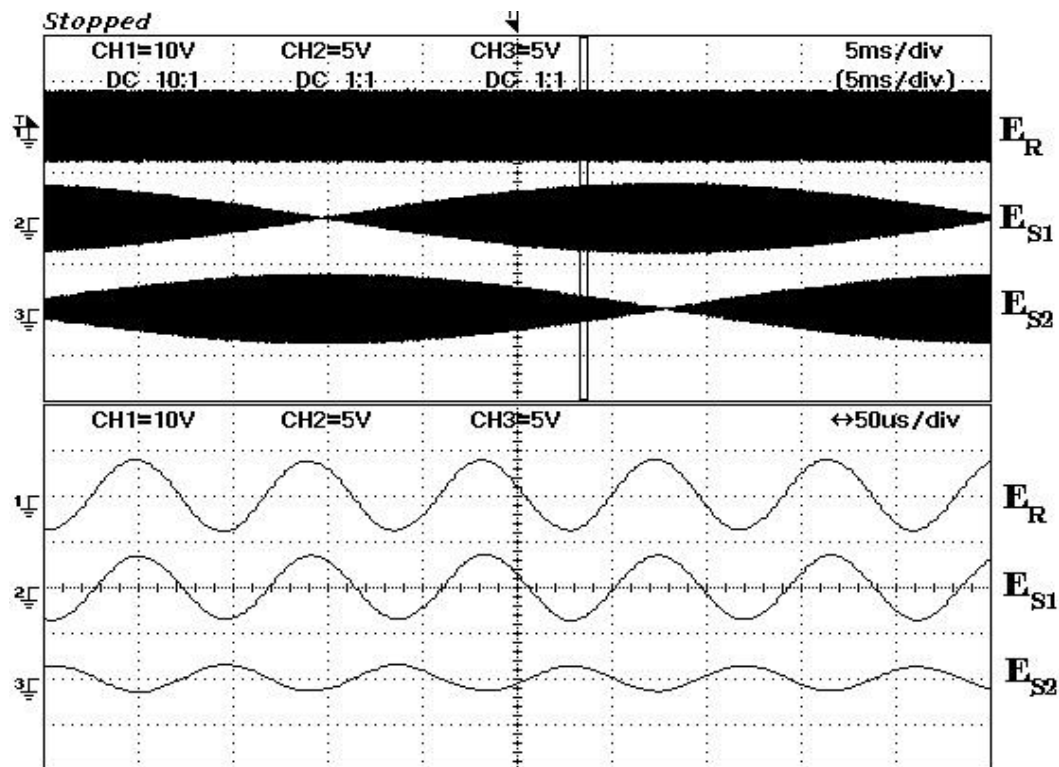


Figure 11. Excitation Voltage and Output of Resolver

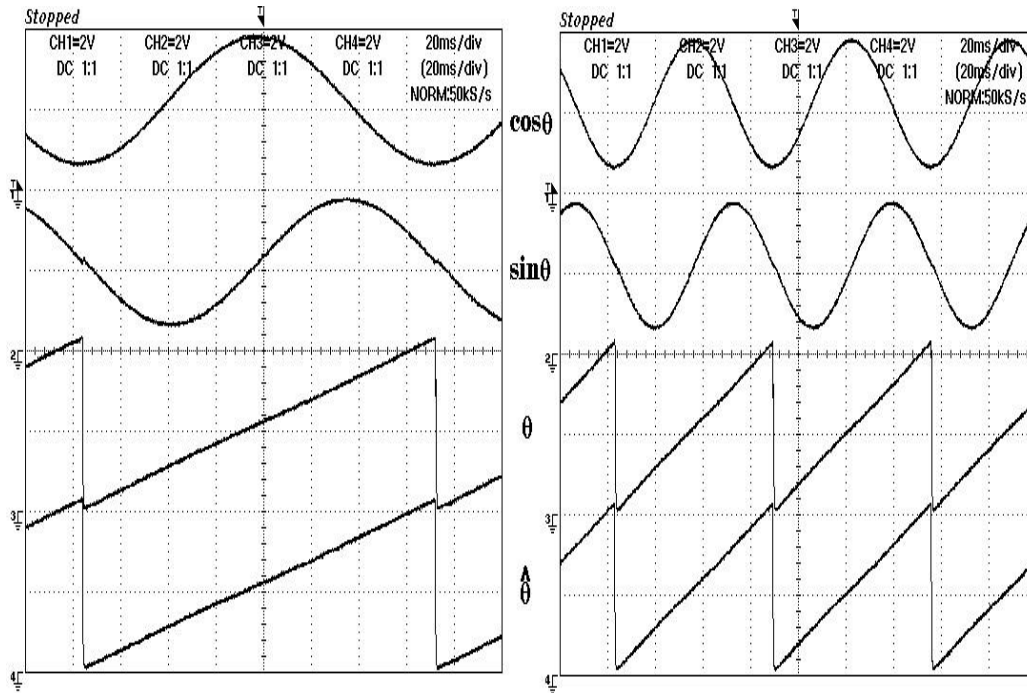


Figure 12. Position Estimation in the Case of Forward Rotation

Coefficients of the equation (22) were determined through repeated experiments, and ω_0 was set to be $2/3$ of the excitation voltage frequency. The waveforms demodulated by the method proposed in Figure 3 are two waveforms on the top in Fig, 12 and Figure 13, and the rotor positions calculated from these two waveforms were measured for the third waveform. The lowest waveform shows the estimated rotor position, and errors for the calculated values and the estimated values could not be determined. Figure 12 corresponds to the case of forward rotation, while Figure 13 corresponds to the case of reverse rotation, showing the waveforms measured for two cases where the rotary speed is high and low.

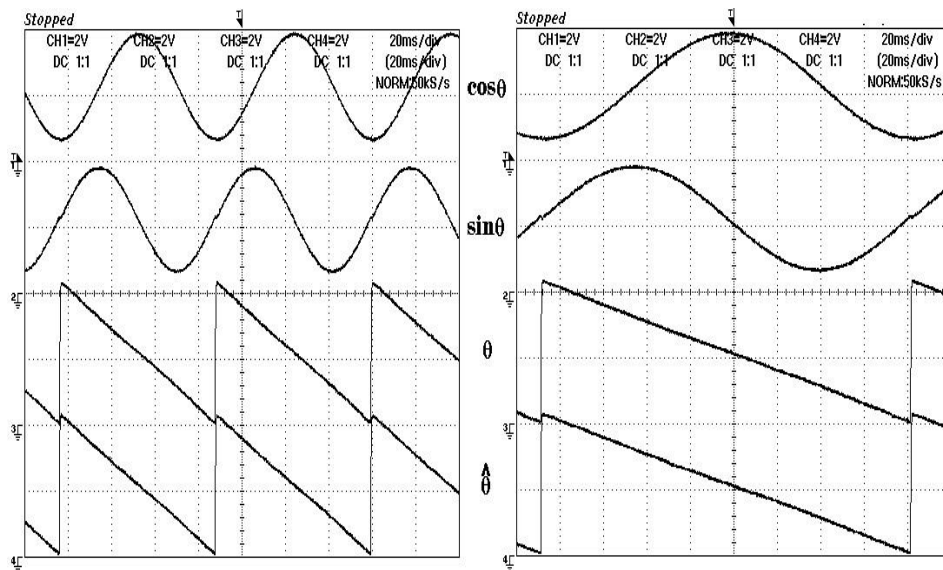


Figure 13. Position Estimation in the Case of Reverse Rotation

Based on the measured waveforms of Figure 12 and Figure 13, it is affirmed that the

use as position information is also possible by processing of analog signals and by direct calculation of angle (\tan^{-1}). When the position calculated by transmitted analog signals and the estimated position were magnified, the measurements as shown in Figure 14 were obtained. According to the observer, removal of noise can be confirmed.

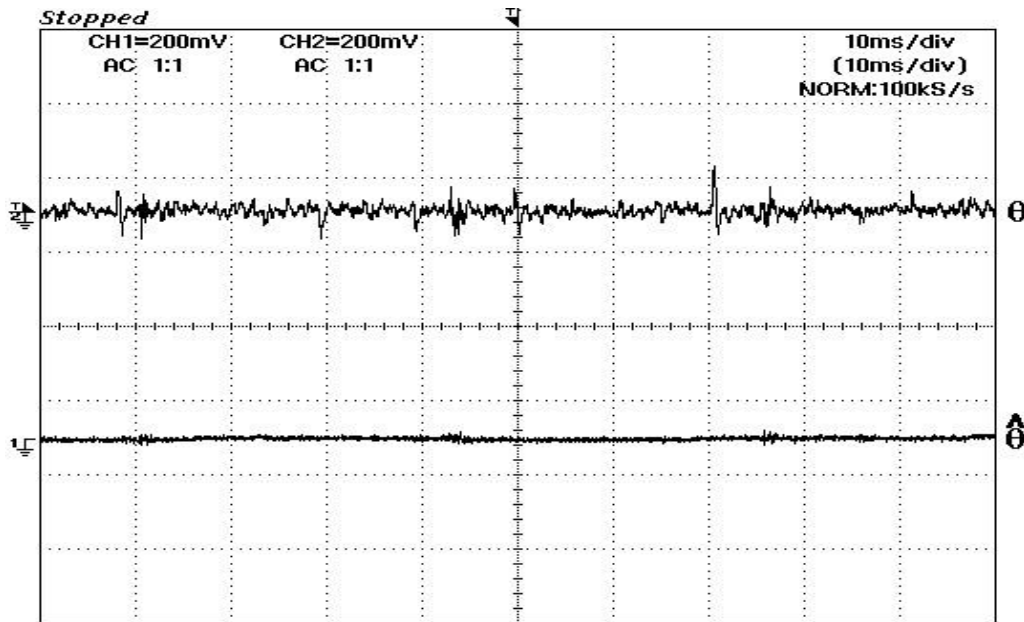


Figure 14. Calculated Position and Estimated Position

6. Conclusion

As a method for varying the speeds by the program in a controller, step response was measured. While the response was being observed, gains of the PI controller as a speed estimator were determined. To the gain of the speed estimator, responsiveness and precision are related. Although it was used as a part of the motor control program, further improvement of precision will be possible if the sampling intervals can be shortened as in the case of dedicated use of the speed detector. According to the experimental results, the stability having a wide range of feedback gain and the feature of rapid convergence as a speed estimator have been confirmed.

Fundamental waves were obtained by DFT for AD-converted data, and from calculation according to which a precision higher than 12 bit was obtained for the position accuracy. Since speed estimation is not related to load conditions, the method is applicable to universal speed detectors or devices with variation in load and inertia.

References

- [1] Young-Choon Kim, Moon-Taek Cho, Ho-Bin Song, Ok-Hwan Kim, "Regeneration Break Control in the High-Speed Area using the Expanding of the Constant Torque Region and Power Region", International Journal of Control and Automation, Vol.6, No.4, August, (2013), pp.347-356.
- [2] Young-Choon Kim, Moon-Taek Cho, "Optimized Design for Electric Vehicle Quick Charging System in Consideration Economic Feasibility", International Journal of Control and Automation, Vol.7, No.4, (2014), pp.235-246.
- [3] Moon-Taek Cho, Young-Choon Kim, Chung-Sik Lee and Ok-Hwan Kim, "Photovoltaics System for Maximum Output Control", International Journal of Control and Automation, Vol.9, No.3, (2016), pp.101-112.
- [4] Y. Toshiaki, S. Shigetomo "Traction Motors Aiming at High Efficiency and Low Maintenance" toshiba review Vol.58, No.9, (2003), pp14-17.
- [5] George Ellis, Jens Ohno Kraha, "Observer-based Resolver Conversion in Industrial Servo Systems.", PCIM 2001, (2001)
- [6] Reza Hoseinnezhad, Peter Harding "A Novel Hybrid Angle Tracking Observer for Resolver to Digital Conversion.", 44th IEEE Conference on Decision & Control, and the European Control Conference, , (2005), pp7020-7025.
- [7] Texas Instruments, "TMS320F240 DSP Solution for Obtaining Resolver Angular Position and Speed.", Application Report SPRA605, February (2000)
- [8] Analog Devices, "12-Bit R/D Converter with Reference Oscillator.", Analog Devices, (2003)

Authors



Young-Choon Kim, He was born in Korea on August 9, 1959. He received the ME.Eng. and Ph.D. degrees from MyongJi Univ. Korea in 1989 and 1997, respectively. Currently, he is an professor in the Kongju National Univ. Dept. of Mechanical & Automotive Eng, Korea. His special field of interest includes power electric, electrical machine, new renewable energy, PSPICE, Fatigue and Fracture Mechanics.



Moon-Taek Cho, He was born in Korea on February 23, 1965. He received the B.S., M. Eng. and Ph.D. degrees from MyongJi Univ. Korea in 1988, 1990 and 1999, respectively. Currently, he is an professor in the Daewon Univ. College Division of Electrical & Electronic Engineering, Korea. His special field of interest includes power electric, electrical machine, new renewable energy, super-capacitor, PSPICE.



Ok-Hwan Kim, He was born in Korea on January 3, 1960. He received the B.S., M. Eng. and Ph.D. degrees from Yonsei Univ. Korea in 1982, 1984 and 1996, respectively. Currently, he is a professor in the Kongju National Univ. Dept. of Mechanical & Automotive Eng., Korea. His special field of interest includes fatigue and fracture mechanics.

